FREQUENCY INSPECTION AS AN ASSESSMENT TOOL FOR THE FROST RESISTANCE OF FIRED ROOF TILES

MARTA KOŘENSKÁ, ZDENĚK CHOBOLA, RADOMÍR SOKOLÁŘ*
PETRA MIKULKOVÁ, JAN MARTINEK

Physics Department, Faculty of Civil Engineering, Brno University of Technology
Žižkova 17, 602 00 Brno, Czech Republic

**Department of Technology of Building Materials and Components, Faculty of Civil Engineering, Brno University of Technology*
Žižkova 17, 602 00 Brno, Czech Republic

E-mail: chobola.z@fce.vutbr.cz

Submitted November 29, 2004; accepted January 4, 2006

Keywords: Frequency inspection, Fired roof tile, Frost resistance

The paper presents the results of the experimental study focused on the application of the frequency inspection method of the assessment of the frost resistance of fired roof tiles. Two sets of fired roof tiles produced by different manufacturing technology were analyzed. For the old-technology-tiles (1988), the consequences of accelerated degradation, which consisted in placing the tiles into a cooling box having a temperature of -70°C, were distinctly apparent immediately after the first cooling cycles. The results were verified by the measurement of the tiles' other properties, such as water absorption, capillarity, and porosity which affect the roof tile frost resistance. The frequency inspection method proves to be a sensitive structure status indicator, which can be used to assessing the frost resistance of the roof tiles. The result show that an advanced technology used for the production of new-technology-tiles (2002) brings an excellent frost resistance and long service tiles life.

INTRODUCTION

The frequency inspection method is one of relatively new product structure testing methods. It is based on the physics of elastic stress wave propagation in bodies. An exciting impulse, being realized, for example, by a mechanical impact on the specimen surface, gives rise to low-frequency stress waves to propagate within the structure and reflect on cracks and the specimen surface. The specimen response to the exciting impulse is picked up on the surface by means of a sensor and transmitted to a computer for frequency analysis. It results in time realization and the corresponding frequency spectrum display. The predominant frequencies (which are represented by local maximum in the spectrum) may be associated with multiple reflections within the structure, carrying information on the structure integrity and defect localization.

The present paper deals with an experimental study of the frequency inspection method applicability to the fired roof tile frost resistance assessment. Our research has addressed two product groups. Group A - fired roof tiles made using the so-called old-manufacturing-technology in 1988; and Group B - fired roof tiles made using the so-called new-manufacturing-technology in 2002, which differs also in raw material structure [1 to 5].

EXPERIMENTAL

In the framework of the accelerated degradation tests, the tiles were let to soak and subsequently placed into a cooling box to be kept there at a temperature of -70°C for 10 minutes. The low-temperature environment was achieved by using liquid nitrogen vapours. Immediately after having been removed from the box, the tiles were dried up in an oven at a temperature of 110°C, to be further exposed to the laboratory temperature for 24 hours to get into equilibrium with the laboratory room temperature. A total of four degradation test cycles have been applied.

The frequency inspection method was applied to the test specimens prior to their degradation and, subsequently, after each degradation cycle in order to keep track of the frequency spectrum variations related to the structure changes.

In order to verify the frequency inspection results and examine their application to the roof tile frost resistance assessment, we have also analyzed some of the tiles' other properties, such as, water absorption, capillarity, and porosity.

To produce the excitation impulse needed for the frequency inspection method application, a metal hammer of a mass of 169 g, hinged in a fixture ensuring a constant release level, y = 2 cm [5], was used to hit the

tile. The tile response to the exciting impulse was picked up by means of a piezoelectric sensor of Sedlák S7 type, whose operating frequencies range from 100 Hz to 50 kHz. The sensor was fitted to the tile surface at a point of coordinates x = 17 cm, y = 9 cm, i.e., at the maximum amplitude point [6]. The response voltage was fed into the input of a Yokogawa DL1540CL digital oscilloscope and further processed by means of a special signal-analysis software package [6].

Physical properties of ceramic materials

The value of absorbed water (NV) indicates the amount of water, related to the desiccated test specimen mass, which has been absorbed by the specimen during the absorption capacity test. There are two kinds of the absorption capacity; atmospheric pressure absorption capacity, NV_1, and boiling point absorption capacity, NV_2 [7].

The specimens were dried out at 110°C and their steady-state mass m_{tr} is measured. Subsequently, upright-standing test specimens were immersed in flowing water while placed in a longitudinal groove in such a way that water level was 50 mm above the tile top edge. The test specimens are left in this water bath for 15 to 18 hours. Furthermore, the specimens were removed from the bath, wiped with a sponge to remove all adhering water from their surface. Finally, their wet mass m_w was determined.

The absorption capacity (%) was calculated by the formula:

$$NV_1 = \frac{m_w - m_{tr}}{m_{tr}} \times 100 \qquad (1)$$

To determine the boiling point absorption capacity NV_2, the specimens were placed on a grid in a boiling pot, while avoiding their contact with the pot walls as well as one to another. The specimen top edge was at least 20 mm under the water surface. During 30-60 minutes, the water was brought to the boil and then kept boiling for 2 hours. Water which evaporates during the boil was replenished steadily to keep the water level over the specimens unchanged. After the boiling was terminated the pot was naturally cooled down to the room temperature. Subsequently, the specimens were taken out from the pot one by one, wiped with a squeezed sponge to be weighed immediately - m_n.

An important piece of information on the specimen porosity is derived from the difference between the various absorption capacities depending on the measuring methods applied. This fact is characterized by the saturated specimen coefficient (*KNS*) - the water penetration coefficient:

$$KNS = \frac{NV_1}{NV_2} \qquad (2)$$

If the water penetration coefficient equals or is less than 0.85, the specimen exhibits good frost resistance.

When a non-sintered ceramic specimen is brought into contact with a liquid, capillary forces will make creeping of liquid into open voids of the specimen, even when opposing the gravity. This feature is called capillarity (*VZ*). The rate of creeping depends mainly on the pore diameter, in other words, on the degree of sintering, on the liquid viscosity, surface tension and the contact angle. The difference in the rate of creeping resulting from different pore arrangement will become most apparent if there are tiny, almost imperceptible, microcracks in the specimen, depreciating its quality. The creeping of liquid through these cracks has considerably higher rate than through other capillary filaments. The rate of creeping may serve as an indication of the so-called the specimen seepage capacity. The limit rate of creeping is 50 mm per 90 minutes [9]. The pore distribution pattern influences substantially the ceramic specimen frost resistance. There are several theoretical models for indirect determination of the specimen frost resistance on the basis of the pore distribution pattern [10].

The closed porosity (PU) is defined as the ratio of the test specimen closed pore volume to the whole test specimen volume (including that of the pores). The actual porosity (PS) indicates the total pore volume in a unit volume of the test specimen. It is an integral value of the pore volume. Following pore-related quantities are of importance for the specimen microstructure porosity evaluation: the pore size, shape and size distribution.

Bentrup [10] have defined the limiting values for the mean pore radii $r_{50\%}$ (i.e., the pore median). Maage [11] has defined the frost resistance in terms of the F factor:

$$F = \frac{3.2}{V} + 2.4 \times P_3 \qquad (3)$$

where V is the total pore volume and P3 is the partial volume of > 3 μm diameter pores in % of the total volume V.

If $F > 70$ and $r_{50\%} > 1$ μm the specimen may be supposed to feature a sufficient frost resistance. On the other hand, if $F < 55$ and is about 1μm, the specimen frost resistance is likely to be very poor.

The widespread measuring methods of the pore properties and dimensions are the intrusion (mercury intrusion) method and the gas adsorption/desorption method. The mercury porosimetry makes possible to measure the volume and size of macropores and mesopores in solids. The measuring method takes advantage of a particular property of mercury, which does not soak most solids (which means that the contact angle between the liquid mercury and the solid exceeds 90°). Due to this fact, mercury penetrates into open pores of a solid under increasing pressure only.

From the volume of mercury intruded into the pores under equilibrium pressure, at which the intrusion took place, the pore volume versus radius distribution can be determined.

In the first step, the tiles were cut up, see figure 1, to be subsequently subject to the above mentioned physical property measurement.

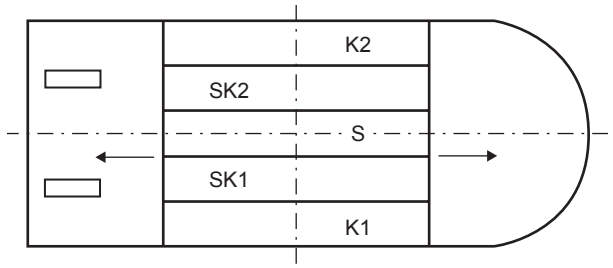

Figure 1. Marking of parts of roof tile.

RESULTS AND DISCUSSION

Figure 2a shows a recording of specimen No. 5 response as picked up at the tile centre by means of S7 sensor. Note that this was the old-technology specimen. This measurement was carried out prior to the low-temperature-treatment induced degradation. Being placed at that point, the sensor picks up the amplitude of the bending vibrations for the most part. The response impulse duration $\tau = 53$ milliseconds. For a $u = u_o \times e^{-\lambda t}$ waveform signal, the attenuation ratio is $\lambda = 58$ s^{-1}.

Figure 3a shows the power spectral density (in relative units) versus frequency plot for specimen No. 5. The predominant frequency appears to be located at $f_o = 2591$ kHz.

Figure 2b shows a response record (in time domain) for specimen No 5 after a single -70°C degradation test cycle application. The corresponding signal response duration is only $\tau = 38$ ms, whereas the attenuation ratio has increased to $\lambda = 128$ s^{-1}.

The spectral density vs. frequency plot (figure 3b) shows that the number of significant frequencies has increased in the range from 1.5 to 5 kHz. The dominant frequency appears to have shifted to $f_1 = 2801$ Hz. The next degradation cycle resulted in the generation of naked-eye-observable cracks, whose width was 0.5 mm to 1 mm almost throughout the tile length.

Figure 3c shows the spectral density plot for the specimens which have been subject to two degradation cycles. The number of significant frequencies has increased significantly in the frequency interval from 1.5 Hz to 5.5 kHz. The dominant frequency appears to have shifted up to $f_2 = 3.198$ Hz, thus being higher by 607 Hz. The attenuation ratio was found to be equal to $\lambda_2 = 385$ s^{-1}. The next degradation cycle resulted in total destruction of the roof tile - the tile broke into two pieces. Table 1 shows the maximum frequencies and attenuation ratios, λ, for specimen No. 5 at different degradation test stages.

Table 1. The dominant frequencies and attenuation ratios for specimen No. 5 at the different degradation test stages.

cycle	attenuation ratio λ (s^{-1})	dominant frequency f (Hz)
0	58	2591
1	128	2801
2	385	3198

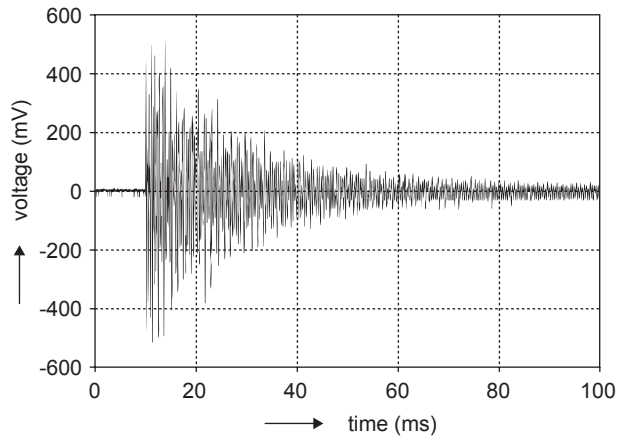

a)

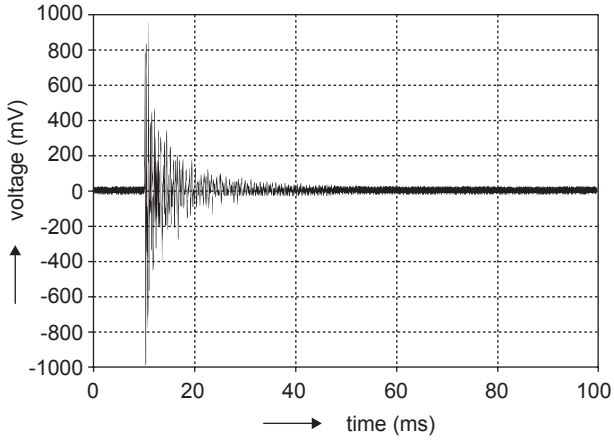

b)

Figure 2. Time-domain response record for a roof tile No.5 fabricated using an old technology. a) before degradation at a temperature of -70°C for 10 minutes, b) after one -70°C degradation test cycle.

Similar power spectral density versus frequency plots for a new-technology-made specimen (B-type) No 24 are shown in figures 4a and 4b. Note that figure 4a shows the pre-degradation status. The attenuation ratio is $\lambda_o = 19\ s^{-1}$ and the dominant frequency is $f_o = 3.234$ Hz. The attenuation ratio value and the dominant frequency shifted to $\lambda_4 = 53\ s^{-1}$ and $f_4 = 3.269$ Hz, i.e., by 35 Hz, respectively, after four -70°C degradation cycles had been applied (figure 8.). It is seen that the dominant frequency shift is rather indistinctive, giving evidence of only minute changes having taken place in the fired roof tile structure, from which a very good frost resistance of these products may be inferred. Table 2 shows the respective maximum frequencies and attenuation ratios, λ, for specimen No 24 and the different degradation test stages.

Figure 5a shows an optical micrograph of the sectional view S, for the old-manufacturing-technology, no-low-temperature-stressed specimen No. 6. Figure 6a presents this specimen's surface. The coarse-grain structure of the surface gives evidence of the raw-material mix preparation method (coarse grinding). There are

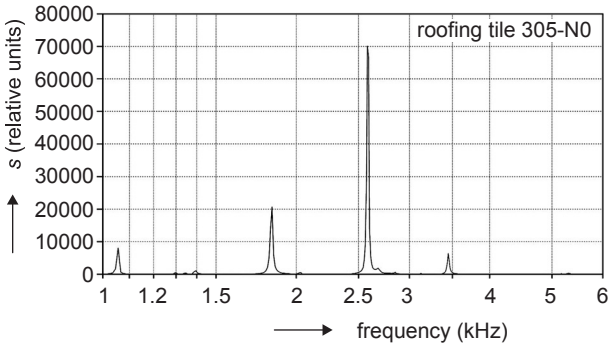

a)

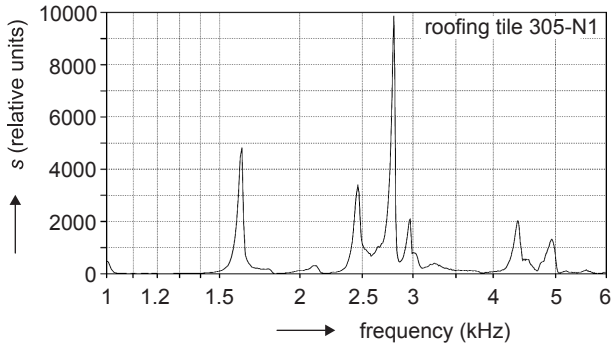

b)

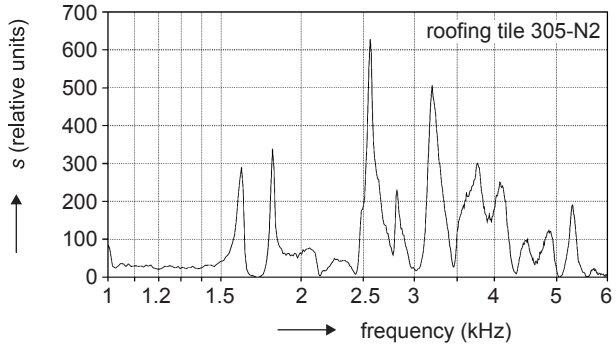

c)

Figure 3. The power spectral density versus frequency plot for specimen No.5 fabricated using an old technology. a) before degradation test, b) after one -70°C degradation test cycle, c) after two -70°C degradation test cycles.

Table 2. The dominant frequencies and attenuation ratios for specimen No. 24 (new technology) at the different degradation test stages.

cycle	attenuation ratio λ (s^{-1})	dominant frequency f (Hz)
0	19	3234
1	22	3239
2	34	3244
3	38	3249
4	53	3269

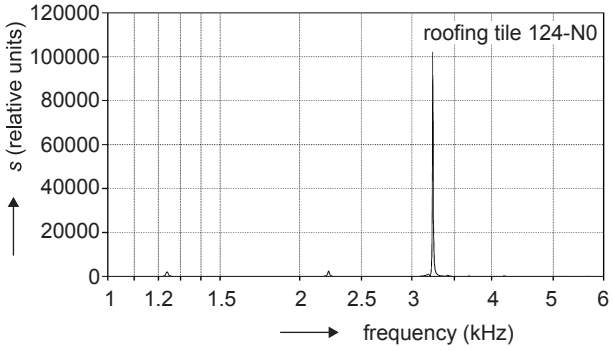

a)

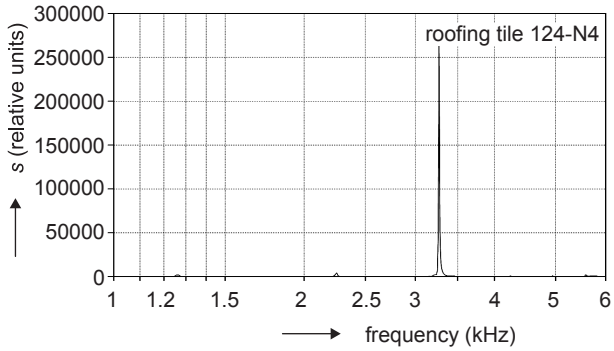

b)

Figure 4. The power spectral density versus frequency plot for specimen No.24, fabricated using a new technology. a) before degradation, b) after four -70°C degradation test cycles.

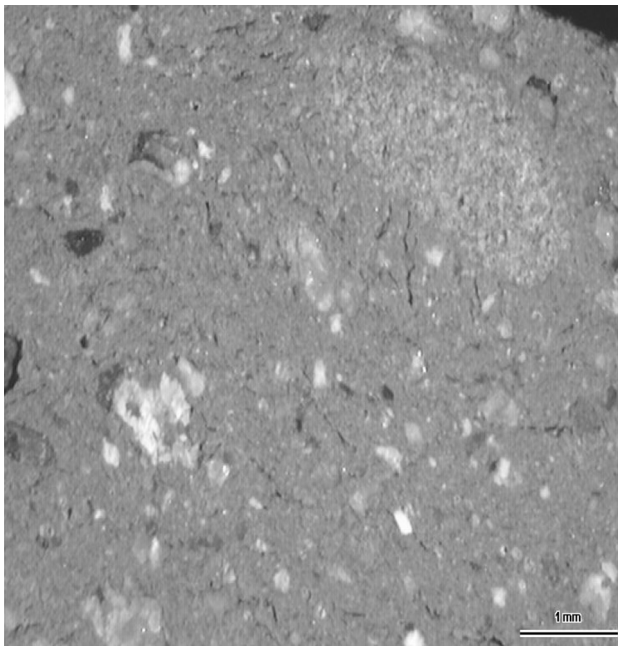

a)

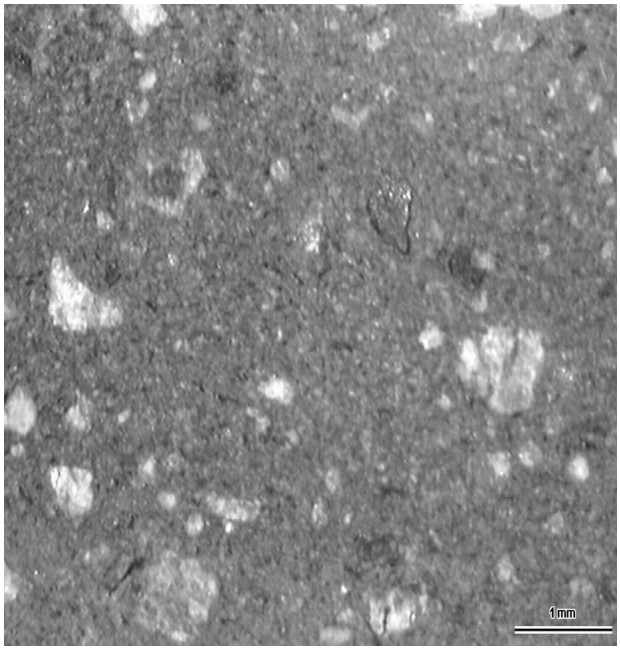

b)

Figure 5. a) The optical micrograph, cut S, for specimen No. 6 fabricated using an old technology, before temperature stress at a temperature of -70°C for 10 minutes. b) The optical micrograph, cut S, for specimen No. 34, fabricated using a new technology, before temperature stress at a temperature of -70°C for 10 minutes.

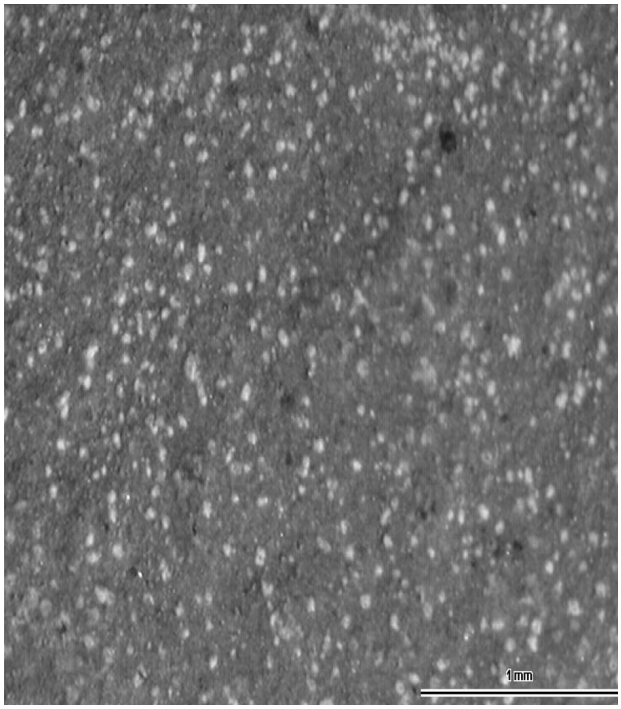

a)

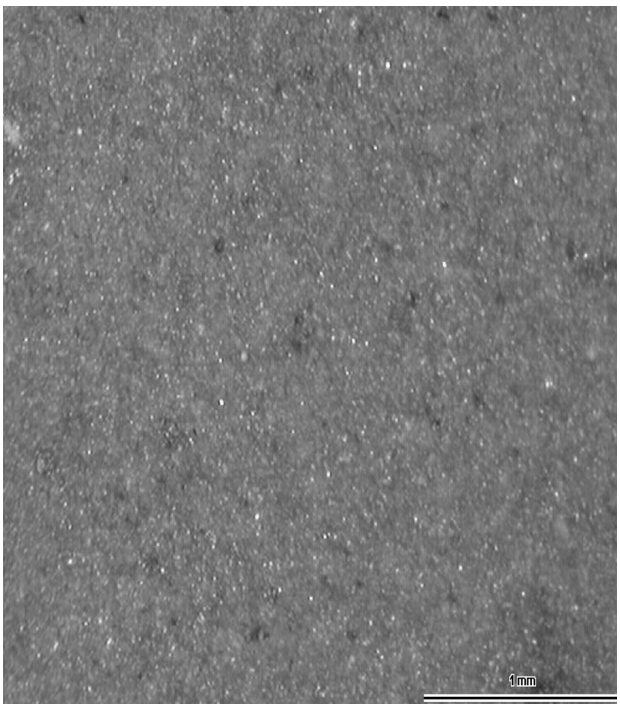

b)

Figure 6. a) Optical micrograph of the specimen No.6, fabricated using an old technology, cut S, before temperature stress. b) Optical micrograph of the specimen No.34, fabricated using a new technology, cut S, before temperature stress.

grains in the structure whose size exceeds 1 mm. The sectional view shows unidirectional texture cracks, which are typical of the worm press grinding method.

Figure 5b shows optical micrograph for a sectional view S, for specimen No. 34, i.e. a new-technology specimen, no low-temperature stressing. Figure 6b shows this specimen's surface.

The results obtained within the framework of this study of capillarity and the water absorption capacity for the old-technology specimen are summarized in table 3, whereas the new-technology specimen' results are in table 4. The lower water absorption capacity for K, K1 and K sections may be attributed to the fact, that these are peripheral cuts, of which at least one edge has not been cut (the cutting operation opens additional soaking pores). The roof tiles differ not only in the technology but also in the raw material composition.

No substantial changes have been found out in the roof tile micro-structure to be due to the extremely low temperature (-70°C) action.

Figure 7 shows a surface photograph of an old-manufacturing-technology-made tile No. 1. An extensive lime nodule can be observed on the roof tile surface. The lime nodule is calcium carbonate which segregates in the material from finely dispersed calcium carbonate. These nodules are harmful after the firing, as it is transformed into calcium oxide. When the specimen

Table 3. Capillarity and the water absorption for the old-technology specimen No.6 and No 1.

specimen	part	NV_1 (%)	NV_2 (%)	*KNS*
6	6K	11.90	14.22	0.84
6	6Z	12.14	14.36	0.85
6	6K2	12.00	14.34	0.84
6	6SK2	12.43	14.63	0.85
6	6S	12.51	14.76	0.85
6	6SK1	12.49	14.52	0.86
6	6K1	12.17	14.20	0.86
1	1K	12.09	14.33	0.84
1	1Z	12.00	14.20	0.85
1	1SK2	12.33	14.41	0.86
1	1S	11.93	14.46	0.83
1	1SK1	12.46	14.49	0.86
1	1K1	11.84	14.05	0.84

Table 4. Capillarity and the water absorption capacity for the new-technology specimen No. 34 and 23.

specimen	part	NV_1 (%)	NV_2 (%)	*KNS*
34	34K	5.56	7.99	0.70
34	34Z	5.67	7.96	0.71
34	34K2	5.59	7.67	0.73
34	34SK2	5.96	8.34	0.71
34	34S	5.81	8.41	0.69
34	34SK1	5.92	8.27	0.72
34	34K1	5.56	7.68	0.72
23	23K	5.69	8.09	0.70
23	23Z	5.73	8.05	0.71
23	23K2	5.39	7.78	0.69
23	23SK2	5.78	8.46	0.68
23	23S	5.83	8.43	0.69
23	23SK1	5.88	8.31	0.71
23	23K1	5.60	7.66	0.73

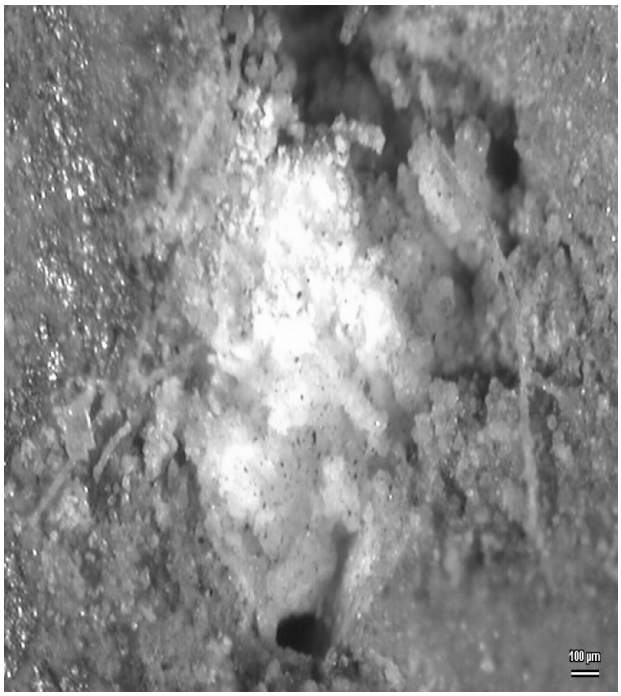

Figure 7. An extensive lime nodule observed on the surface of the sample No. 1 - old technology fired roof tile.

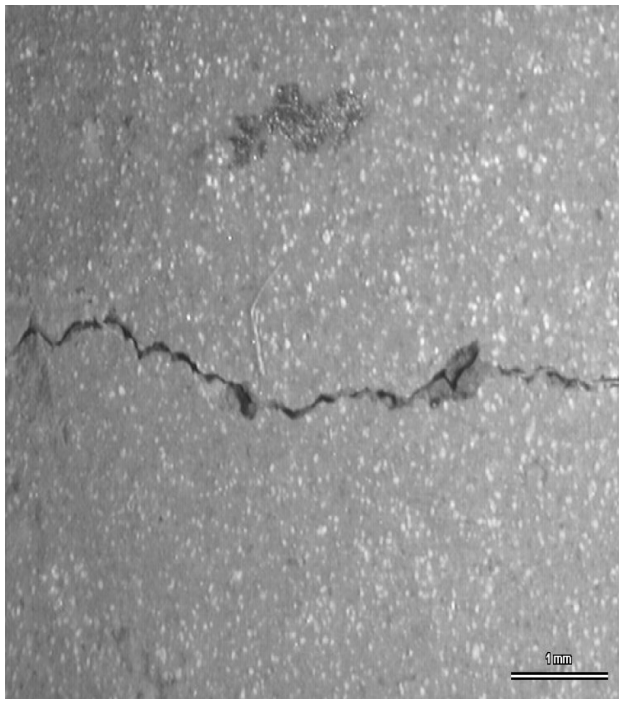

Figure 8. The crack of a length of 5 cm appeared in specimen No.1 - old technology fired roof tile.

is exposed to the air moisture, the calcium oxide is formed calcium hydroxide, which then increases in volume by 70 % to 90 %. This volume expansion elevates pressure in the specimen, which can damage the product by giving rise to scaling or crack generation.

The next photograph, figure 8 shows a pronounced crack of a length of 5 cm, which was observed to occur in specimen No. 1 after 5 low-temperature (-70°C) stress cycles had been applied to it. It was an old-technology-made roof tile.

The new-technology tiles feature a capillarity ranging from 37 mm/90 min to 39 mm/90 min. These figures are contrasting with those of the old-technology tiles, 70 mm/90 min to 75 mm/90 min, exceeding significantly very high probability of the specimen frost resistance. The water penetration coefficient, KNS, equals 0.83 to 0.86 for the old-technology tiles, being on the very margin of the frost resistance acceptability. It equals 0.68 to 0.73 for the new-technology tiles, thus guaranteeing a very good frost resistance.

The results gained from the high-pressure porosimetry application are shown in table 5. It is seen that the old-technology tiles do not meet the frost resistance requirements. This statement can be inferred from the high pore volume, 147.2 mm^3/g, as well as the value of F = 49, and, consequently, the low value of $r_{50\%}$ = = 0.55 μm. On the contrary, the new-technology roof tiles achieve much more favourable values, promising very good frost resistance figures. The pore volume is 86 mm^3/g, the factor F = 104 and $r_{50\%}$ = 1.12 μm.

The pore size distribution measurement results are presented in figure 9.

Table 5. Parameters from high-pressure mercury porosimetry. Old-technology specimen No.1 and new-technology specimen No.34.

	No. 1	No. 2
Volume of pores (mm^3/g)	86.2	147.2
Apparent density (kg/m^3)	2600	2685
Volumes mass (kg/m^3)	2125	1925
Apparent porosity (%)	18.3	28.3
F	104	49
$r_{50\%}$ (m)	1.12	0.55

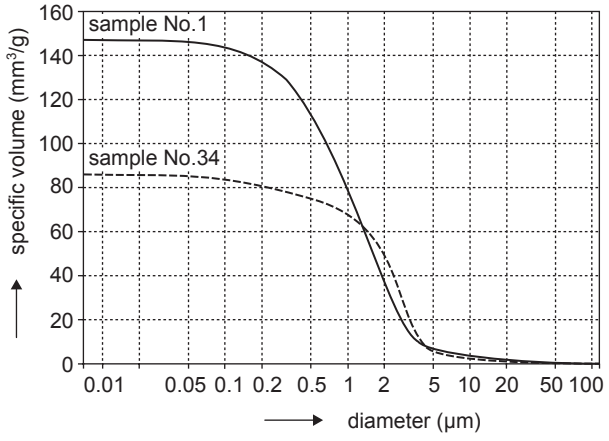

Figure 9. Distribution of the existing pores in ceramic bodies. Old-technology specimen No.1 and new-technology specimen No.34.

CONCLUSION

Our experiments have been aimed at examining the frost resistance assessment methods of fired roof tiles on the basis of the frequency inspection. Two fired roof tile sets have been tested. Group A - the roof tiles made using the old-manufacturing-technology in 1988; and Group B - the roof tiles made using the new-manufacturing-technology in 2002.

The tiles were subject to accelerated degradation tests consisting in cooling to a temperature of -70°C. The dominant frequencies proved to shift upwards during the degradation tests.

The A-type specimens - old technology - have shown an increase in the number of dominant frequency components present and a pronounced maximum frequency shift of up to several thousand Hz, which was due to the structure defects induced by the degradation cycle application.

The B-type specimens - new technology - the dominant frequency number remains unchanged, the frequency shift being very low, several decades of Hz only, which gives evidence of the fact that the degradation cycle application did not result in significant specimen structure defects.

To verify that the above mentioned structure changes are really responsible for the tile frost resistance, some other tile properties, which are considered to be also connected with their frost resistance, such as, the water absorption capacity, capillarity and porosity, have been measured, too. Our results confirm that the old-technology tiles exhibit very poor frost resistance and a fast degradation process, contrasting with the new-technology tiles, for which we may expect - based on our experiment results - very good frost resistance and only insignificant accelerated degradation induced structural changes.

Our measurements also show that the frequency inspection method is a sensitive structure status indicator, which can also be used to assess the frost resistance of these building elements.

The main benefit resulting from the application of this method, compared with the applicable ČSN EN 539-2 standard-based frost resistance test currently in use, is a higher sensitivity to the defect occurrence, higher application rate and interpretation simplicity.

Changes, which could not be observed visually, are recorded and the human factor effecting the test evaluation is eliminated. After-test time consuming and subjective visual evaluation are eliminated. This experiment represents a new approach to the fired roof tile frost resistance tests.

Acknowledgement

This research has been supported by project of GACR No.103/05/2683 and by project of GACR No.103/03/0295.

References

1. Korenska M., Chobola Z., Mikulkova P., Martinek J.: *Proc. of the Fourth Conf. Material Problems in Civil Engineering MATBUD´2003*, p.239-244, Krakow University of Technology Poland, Wydavnictvo Politechniki Krakowskiej Dzial - Poligrafii, Krakow 2003.
2. Korenska M., Chobola Z., Mikulkova P., Martinek J.: Proc. of 33rd International Conference, Defektoskopie 2003, p. 105-110, Czech Society for Non-destructive Testing, Ostrava 2003.
3. Martinek J., Mikulkova P., Chobola Z.: Proc. of International Workshop on Physical and Material Engineering 2003, p. 161-164, Slovak University of Technology, Bratislava 2003.
4. Mikulkova P., Korenska M., Martinek J., Chobola Z.: Proc. of International Workshop on Physical and Material Engineering 2003, p. 145-148, Slovak University of Technology, Bratislava 2003.
5. Chobola Z., Mikulkova P., Martinek J.: Proc. of. the Workshop NDT CMC 2003 Non-Destructive Testing of civil Engineering Structures and Constructions, p. 36-41, Technical University of Brno, Brno 2003.
6. Martinek J., Chobola Z.: Proc. of International Workshop on Physical and Material Engineering 2003, p. 149-152, Slovak University of Technology, Bratislava 2003.
7. Lach V.: Keramika/Ceramics, VUT Brno 1989.
8. Lach V.: Keramika/Ceramics, VUT Brno 1992.
9. Hanykýř V., Kutzendorfer J.: Technologie keramiky, Vega, Hradec Králové 2000.
10. Bentrup H., Franke L.: Ziegelindustrie International No. 7-8, p. 483; No.9, p. 528, (1993). Friese, P. Predictions Ziegelindustrie International, No. 12, p. 952, (1995).
11. Maage M.: Ziegelindustrie International, No. 9, p. 472, No.10, p. 582, (1990).

FREKVENČNÍ INSPEKCE JAKO METODA PRO POSOUZENÍ MRAZUVZDORNOSTI PÁLENÝCH STŘEŠNÍCH KRYTIN

MARTA KOŘENSKÁ, ZDENĚK CHOBOLA, RADOMÍR SOKOLÁŘ, PETRA MIKULKOVÁ-TREBULÁKOVÁ, JAN MARTINEK

Ústav fyziky
Stavební fakulta, Vysoké učení technické Brno,
Žižkova 17, 602 00 Brno

V předloženém článku jsou prezentovány výsledky experimentálního studia zaměřeného na využití metody frekvenční inspekce pro posouzení mrazuvzdornosti pálených střešních krytin. Analyzovány byly dva soubory pálených střešních tašek. Jednalo se o tašky vyrobené starou technologií v roce 1988 a novou technologií v roce 2002. U tašek zhotovených starou technologií byly důsledky zrychlené degradace vyvolané uložením máčených tašek do chladícího boxu s teplotou -70°C patrné již po prvních cyklech. Pro možnost verifikace výsledků získaných metodou frekvenční inspekce byly proměřeny také některé další fyzikální vlastnosti testovaných pálených střešních tašek související s odolností proti mrazu: nasákavost, vzlínavost a pórovitost. Bylo ověřeno, že metoda frekvenční inspekce je citlivým indikátorem stavu struktury a lze ji využít k posuzování mrazuvzdornosti střešních krytin. Rovněž bylo ukázáno, že tašky vyrobené novou technologií vykazují výrazně vyšší odolnost proti mrazu.